

(12) PATENT
(19) AUSTRALIAN PATENT OFFICE

(11) Application No. AU 199718170 B2
(10) Patent No. 702009

(54) Title
Screw thread implant

(51)⁶ International Patent Classification(s)
A61C 008/00

(21) Application No: **199718170** (22) Application Date: **1997.02.12**

(87) WIPO No: **WO97/29713**

(30) Priority Data

(31) Number (32) Date (33) Country
9600517 **1996.02.13** **SE**

(43) Publication Date : **1997.09.02**
(43) Publication Journal Date : **1997.10.30**
(44) Accepted Journal Date : **1999.02.11**

(71) Applicant(s)
Astra Aktiebolag

(72) Inventor(s)
Stig Hansson

(74) Agent/Attorney
E F WELLINGTON CO

(56) Related Art
WO 93/06786
WO 94/09717

OPI DATE 02/09/97 APPLN. ID 18170/97
AOJP DATE 30/10/97 PCT NUMBER PCT/SE97/00212



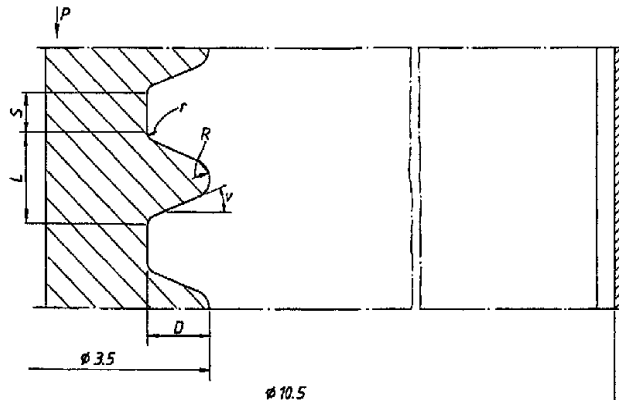
AU9718170

WO 97/29713

(51) International Patent Classification 6 : A61C 8/00	(11) International Publication Number: WO 97/29713
A1	(43) International Publication Date: 21 August 1997 (21.08.97)

(21) International Application Number: PCT/SE97/00212	(81) Designated States: AL, AM, AT, AU, AZ, BA, BB, BG, BR, BY, CA, CH, CN, CU, CZ, DE, DK, EE, ES, FI, GB, GE, HU, IL, IS, JP, KE, KG, KP, KR, KZ, LC, LK, LR, LS, LT, LU, LV, MD, MG, MK, MN, MW, MX, NO, NZ, PL, PT, RO, RU, SD, SE, SG, SI, SK, TJ, TM, TR, TT, UA, UG, US, UZ, VN, YU, ARIPO patent (KE, LS, MW, SD, SZ, UG), Eurasian patent (AM, AZ, BY, KG, KZ, MD, RU, TJ, TM), European patent (AT, BE, CH, DE, DK, ES, FI, FR, GB, GR, IE, IT, LU, MC, NL, PT, SE), OAPI patent (BF, BJ, CF, CG, CI, CM, GA, GN, ML, MR, NE, SN, TD, TG).
(22) International Filing Date: 12 February 1997 (12.02.97)	
(30) Priority Data: 9600517-8 13 February 1996 (13.02.96) SE	
(71) Applicant (for all designated States except US): ASTRA AKTIEBOLAG [SE/SE]; S-151 85 Södertälje (SE).	
(72) Inventor; and	Published
(75) Inventor/Applicant (for US only): HANSSON, Stig [SE/SE]; Gäsmossen 32, S-436 39 Askim (SE).	With international search report.
(74) Agent: ASTRA AKTIEBOLAG; Patent Dept., S-151 85 Södertälje (SE).	

(54) Title: SCREW THREAD IMPLANT



(57) Abstract

The present invention relates to a thread or oriented macroroughness for bone implants, particularly threaded dental implants, a section of said thread or roughness (i.e. the profile) comprising two flanks, a top radius R at the apex formed by the intersection of said two flanks, a bottom radius r formed at the bottom of the groove between two adjacent threads or roughnesses, said flanks forming an angle v with a plane which is perpendicular to a cross section of said thread or roughness and perpendicular to the surface of the implant body, said profile further having a height D. According to the invention the dimensions of the thread or roughness are subject to the following restrictions: for $10^\circ \leq v < 35^\circ$, R is greater than $0.4 \times D$ and that, for $35^\circ \leq v \leq 55^\circ$, R is greater than $0.2 \times D$. In a preferred embodiment the restrictions are: for $0.05 \text{ mm} \leq D \leq 0.5 \text{ mm}$ and $35^\circ \leq v \leq 55^\circ$, the top radius R is larger than $0.2 \times D$ but smaller than D, and in that, for $0.25 \text{ mm} \leq D \leq 0.5 \text{ mm}$ and $10^\circ \leq v < 35^\circ$, R is greater than $0.4 \times D$ but smaller than D.

SCREW THREAD IMPLANT

The present invention relates to implants for implantation into bone, in particular to dental implants, said implants being provided with threads or an oriented macroroughness. The term "oriented macroroughness" should be 5 understood to comprise elongated beads which may be continuous or not, which may be oriented along the periphery of a cross-section of the implant or not. The oriented macroroughness should have a cross-section or profile specified in the way the thread profile will be defined below and in the appended claims.

10 Background to the invention

Bone implants are normally made of rigid material, mostly of titanium, which has been shown to have an affinity for bone tissue and which has an excellent biocompatibility. Bone implants often have a cylindrical, threaded shape and are screwed into bore-holes in the bone tissue which may be pre-tapped or 15 not.

Under certain conditions titanium implants attain a close apposition with the bone tissue which sometimes is called osseointegration. Some factors determining the tissue response to a bone implant have been found to be the following: the biocompatibility of the implant material, the implant design, the 20 implant surface, the status of the host bed, the surgical technique and the loading conditions. As far as the implant design is concerned, a review of the dental implant literature reveals that implants of a large number of different shapes have been used in the past. It appears as if new implant designs to a great extent have been introduced and evaluated on a trial and error basis. As 25 the reason for an implant failure is multi-factorial, a good design may have been discarded due to for example an improper surgical technique or improper loading conditions. Titanium screw-shaped dental implants were used early in the 1960's, those implants do not appear to have been a success; possibly due to the reasons mentioned above.

30 Overloading has been identified as a main etiologic factor behind loss of dental implants today. If bone is subject to extreme stress it will be resorbed.

- 2 -

Assuming that stress induced bone resorption is triggered off when the stresses reaches a certain level, an implant should have such a design that the maximum stresses arising in the bone, as a result of a certain load, is minimized.

5 Screw-shaped titanium dental implants dominate the market today. Several studies have addressed the relation between macroscopic design and holding power of screws in bone. By far most of them have been made within the orthopaedic discipline and have had an experimental approach. Pullout tests were carried out in the 1950's on dog femurs and tibias using vitallium
10 bone screws with different thread profiles. It was observed that when pulling out a freshly inserted screw, the bone threads did not strip but the screw pulled out a small cone-shaped button of compact bone. Clinical experience shows that a bone plate and its screws are sometimes avulsed from bone. This avulsion is preceded by bone resorption. The opinion has been expressed
15 that such a loss of holding power is caused by mechanical factors. Continuous compression of cancellous bone by screw threads has been shown to result in hypertrophy and realignment of the trabeculae in parallel with the force. It has also been claimed that cortical bone subjected to compression retains its integrity and is not resorbed.

20 The relevance of pull-out experiments can however be doubted. In a pull-out test acute fracture is provoked. Dental implants seldom fail by acute fracture of the supporting bone. On the contrary the fracture of the implant-bone interface is normally the end of a long process of marginal bone resorption. As mentioned above, the assumption that stress induced bone
25 resorption is triggered off when the stresses reaches a certain level implies that an implant should be given such a design that the stress peaks arising in the bone are minimized.

30 It has been found that a bone implant being provided with threads or an oriented macro-roughness intended to transfer loads to the bone tissue and designed in accordance with the appended main claim minimizes the stress peaks in the surrounding bone tissue. Preferred embodiments are set forth in the dependent claims.

Short description of the appended drawings

Fig 1 illustrates a profile of a thread or roughness according to the invention;

Fig 2 illustrates the so called contact elements on the profile;

5 Fig 3 illustrates the model used to calculate the stresses;

Figs 4 and 5 show the distribution of the elements around the profile of a profile according to the invention respectively a prior art implant

Fig 6 illustrates the location of the different maximal stresses.

Fig 7 illustrates an alternative embodiment of the apex of the thread

10 Detailed description of a preferred embodiment of the invention

Fig 1 illustrates how the parameters describing the profile according to the invention are defined. The implant shown is a screw-shaped dental implant with a diameter of 3.5 mm.

The thread profile has two thread flanks and the height of the thread is
15 D. The top radius formed at the apex of the thread profile at the intersection of the two thread flanks is designated R, and the bottom radius between two adjacent thread profiles r. The thread flanks form an angle v with a plane which is perpendicular to a cross-section of the thread and perpendicular to the surface of the implant body. The distance L is defined as the distance
20 between the points of intersection between the two flanks on a thread and the surface of the implant body, the surface of the implant body being defined as the cylindrical surface touching the deepest parts of the threads.

A standard prior art screw-shaped implant with an overall diameter of 3.5 mm would typically be provided with threads having a height D of about
25 0.35 mm, a flank angle v of 30°, a top radius R of about 0.065 mm corresponding to about 0.2xD and bottom radius of about 0.05 mm corresponding to about 0.15xD.

As discussed above, the object of the invention is to equalize and minimize the stress concentrations in the bone tissue which are a result of
30 the loads on the implant in order to obtain an even stress distribution in the bone tissue so as to avoid resorption of the bone tissue because of high

stress concentrations whilst avoiding low stresses that also might cause bone tissue resorption.

In accordance with the invention it has been found that screw threads (macro-roughness) either having a top radius exceeding $0.4xD$ or a flank angle exceeding 35° substantially equalizes the stress distribution in the bone tissue surrounding the implant. More particularly, the top radius R should be larger than $0.2xD$ and smaller than D for $35^\circ \leq v \leq 55^\circ$ and $0.05 \leq D \leq 0.5$ mm and larger than $0.4xD$ and smaller than D for $10^\circ \leq v < 35^\circ$ and $0.25 \leq D \leq 0.5$ mm.

10 An embodiment which at present seems most promising is an embodiment wherein $0.03 \leq R \leq 0.05$ mm, $37^\circ \leq v \leq 43^\circ$, $0.01 \leq r \leq 0.025$ and $0.08 \leq D \leq 0.15$.

15 The following calculations illustrate this point. The calculations are performed by means of finite element analysis. The theory of elasticity according to Timoshenko is applied. The program used is Ansys revision 5.0.

The object studied is a vertically oriented screw-like implant with a major diameter of 3.5 mm. This implant is built up of identical axisymmetric elements where each element corresponds to one pitch height of a screw. The thread is modeled as a ring on each element. The profile of the thread as seen 20 in Fig. 1 is characterized by the thread depth (D), the top radius (R), the flank angle (v), the bottom radius (r) and a straight part of the length S at the bottom of the thread. The length of the curved part of such an element is, as defined above, designated L . The straight part of the length (S) was set as a coefficient c multiplied with this length ($S = c \cdot L$). Calculations were made 25 for values of the thread depth of 0.1 mm, 0.2 mm, 0.3 mm and 0.4 mm while the value of the top radius was set as a coefficient multiplied with the thread depth. The value of this coefficient was set at 0.1, 0.2, 0.4, 0.6, 0.8 and 1. The flank angle was varied between 0° and 60° with an increment of 10° . The bottom radius was set at 0.1 times the thread depth. The coefficient c 30 was set at 0, 0.2, 0.4, 0.8 and 1.6. This means that a total of $4 \times 6 \times 7 \times 5 \times 1 = 840$ different thread profiles are used. The implant was assumed to be infinitely long and was assumed to be completely embedded in cortical bone.

- 5 -

100% bone apposition was assumed. The bone was assumed to be attached to the inner wall of an outer cylinder with a diameter of 10.5 mm, see Fig. 1. Rotational symmetry was further assumed. The implant and the outer cylinder were assumed to be infinitely stiff while the bone was assumed to be a continuum material, isotropic and linearly elastic with a modulus of elasticity (Young's modulus) of 150 GPa and a Poisson's ratio amounting to 0.3. It was assumed that the bone-implant interface was frictionless and that only compressive forces could be transmitted between the implant and the bone. These interface conditions are modeled by means of contact elements, the lines adjacent to the thread surface in Fig. 2. As is evident from fig. 2 parts of the interface does not have contact elements, the reason being that the interfacial bone at these locations in test runs had turned out to retreated from the implant.

An infinitely big axial load (a finite load per screw element) was applied on the infinitely long implant. With the assumptions made, the same mechanical events (stresses, strains, displacements) will occur in the bone outside all elements of which the infinitely long implant is composed. Consequently it is sufficient to study one single element of the implant, including the surrounding bone, provided that proper boundary conditions can be set up wherein this element with its surrounding bone borders to the overlying and underlying counterparts. The boundary conditions which were used were that, when the load was applied, all nodes in the bone lying in the horizontal plane defined by the upper limiting surface of the element in couples underwent the same displacements as the corresponding nodes in the bone lying in the horizontal plane defined by the lower limiting surface of the same element (Fig.3).

The load, F , which was transmitted from the implant element into the bone tissue was set as a constant (k) multiplied with the length ($L + S$) of the implant element which latter was dependent upon the top radius, the flank angle, the bottom radius, the thread depth and the length of the straight part if any. The information sought was the maximum tensile stress, the maximum compressive stress and the maximum von Mises stress in the bone as a

function of the values of the variables used. The implant element was modeled to be completely stiff and fixed, the load \mathbf{F} being applied at the further end of the bone as is shown in Fig. 3.

The element mesh was built up parametrically. In fig. 4 and 5 the 5 element mesh close to the implant is shown for two calculation examples called *Parameter set 1* and *Parameter set 2*. Parameter set 1 corresponds to a thread profile according to the invention with $D = 0.1$ mm, $v = 40^\circ$ and $R = 0.4xD$, $r = 0.1xD$ whereas parameter set 2 largely corresponds to the prior art implant given above. Each element contained four nodes, the number of 10 degrees of freedom for each node being two. The number of elements used in the mesh varied with the length of the straight portion at the bottom of the thread expressed by the coefficient c . With a value of the coefficient c of 0, 0.2-0.4 and 0.8-1.6 the number of elements were 1129, 1305 and 1481 respectively.

15 It is assumed that the screw-like structure was embedded in cortical bone. The following mean values for the ultimate stress of human cortical bone have been obtained empirically: $\sigma_{uo}^+ = 133$ MPa, $\sigma_{uo}^- = 193$ MPa, $\sigma_{u90}^+ = 51$ MPa and $\sigma_{u90}^- = 133$ MPa where the ultimate stress in regard of tension and compression is denoted by σ_u^+ and σ_u^- respectively. σ_{uo} and σ_{u90} signify 20 ultimate stresses in parallel with the long axis of the bone respectively in a transversal plane. It is natural to allow bone stresses of different kinds in proportion to the ultimate stress. The ratios $\sigma_{uo}/\sigma_{uo}^+$ and $\sigma_{u90}/\sigma_{u90}^+$ are according to the above 1.45 and 2.61 respectively. In order to simplify 25 comparisons with the maximum tensile stresses obtained the ratios $\sigma_{max}^-/1.45$ and $\sigma_{max}^-/2.61$ are presented in the results (tables 1-4 and 9-12). However, for the calculations, the ratio $\sigma_{max}^-/2$ is the value which is of most interest.

Disregarding the von Mises stress, the combination of values of the profile parameters which minimizes the highest of the values, σ_{max}^+ and $\sigma_{max}^-/2$ may be regarded as the most favourable thread design.

30 The von Mises stress can be expressed by the formula
$$\sigma_v = \sqrt{\sigma_1^2 + \sigma_2^2 + \sigma_3^2 - \sigma_1\sigma_2 - \sigma_2\sigma_3 - \sigma_1\sigma_3}$$
 where σ_1 , σ_2 and σ_3 are the principal stresses. This formula does not take into

consideration a situation where the compressive stress of a material differs from the tensile stress. An analysis of the results showed that the maximum von Mises stress regularly was composed of one high compressive principal stress, one compressive stress of intermediate magnitude and one 5 insignificant tensile principle stress. In order to be directly comparable with the maximum tensile stress the maximum von Mises stress should, as the maximum compressive stress, be divided with a certain factor. It is obvious that the value of this factor lies between 1.45 and 2.61 (it never attains the value 1.45 nor does it attain the value 2.61). For that reason the ratios 10 $\sigma_{e,max}/1.45$ and $\sigma_{e,max}/2.61$ are presented in the results in tables 1-4 and 9-12 below. The von Miese's stresses are given for comparative purposes.

Tables 1 - 4 show the results of the calculations. As can be seen in the tables, the values for $\sigma_{e,max}^+$ generally are less than 2 and for $\sigma_{max}/1.45$ generally are less than 2.75 (which corresponds to a value also less than 2 for 15 $\sigma_{max}/2$) within the rectangles which are drawn with dashed lines in table 1 only but are to correspond to the fields $0.05 \text{ mm} \leq D \leq 0.5 \text{ mm}$ and $35^\circ \leq v \leq 55^\circ$, the top radius R being larger than $0.2xD$ but smaller than D; $0.25 \text{ mm} \leq D \leq 0.5 \text{ mm}$ and $10^\circ \leq v < 35^\circ$, R being greater than $0.4xD$ but smaller than D. The calculation results for the parameter fields in which 20 $\sigma_{e,max}^+ < 2$ and $\sigma_{max}/2 < 2$ are illustrated with full lines in the tables.

As clearly can be seen, the standard screw-shaped implant falls outside these parameter fields.

Tables 5 - 8 illustrate the effect obtained by the introduction of a distance S between two adjacent threads. The part of the distance S which is 25 straight is given as a coefficient to be multiplied with the length L, i. e. the distance defined above between the points where the flanks intersect the body of the implant. If the coefficient is 0 there is no positive effect of the introduction of a straight part. As can be seen, the positive effects mainly occur for small flank angles and for relatively large top radii, the parameter 30 fields being shifted slightly to lower top radii for small flank angles as for instance can be seen by comparing tables 3 and 11.

Tables 9 - 12 show the minimum values for σ_{\max}^+ and the corresponding $\sigma_{\max}^-/1.45$ corresponding to the values given in tables 5 - 8.

Some preferred embodiments are given in the following lists.

5	Top radius	Flank angle	Bottom radius	Thread height(D)	Straight part at bottom
1	0.03-0.05	37°-43°	0.01-0.025	0.08-0.15	0
10	2	0.2D-1.0D	35°-55°	0 -0.2D	0.05-0.15
	3	0.2D-1.0D	35°-55°	0 -0.2D	0.05-0.15
	4	0.2D-1.0D	35°-55°	0 -0.2D	0.05-0.15
	5	0.2D-1.0D	35°-55°	0 -0.2D	0.15-0.25
15	6	0.2D-1.0D	35°-55°	0 -0.2D	0.15-0.25
	7	0.2D-1.0D	35°-55°	0 -0.2D	0.15-0.25
	8	0.2D-1.0D	35°-55°	0 -0.2D	0.25-0.35
	9	0.2D-1.0D	35°-55°	0 -0.2D	0.25-0.35
20	10	0.2D-1.0D	35°-55°	0 -0.2D	0.25-0.35
	11	0.2D-1.0D	35°-55°	0 -0.2D	0.35-0.50
	12	0.2D-1.0D	35°-55°	0 -0.2D	0.35-0.50
	13	0.2D-1.0D	35°-55°	0 -0.2D	0.35-0.50
25	14	0.2D-1.0D	35°-55°	0.2D-1.0D	0.05-0.15
	15	0.2D-1.0D	35°-55°	0.2D-0.8D	0.05-0.15
	16	0.2D-1.0D	35°-55°	0.2D-0.6D	0.05-0.15
30	17	0.2D-1.0D	35°-55°	0.2D-1.0D	0.15-0.25
	18	0.2D-1.0D	35°-55°	0.2D-0.8D	0.15-0.25
	19	0.2D-1.0D	35°-55°	0.2D-0.6D	0.15-0.25

- 9 -

20	0.2D-1.0D	35°-55°	0.2D-1.0D	0.25-0.35	0
21	0.2D-1.0D	35°-55°	0.2D-0.8D	0.25-0.35	0-1D
	22	0.2D-1.0D	35°-55°	0.2D-0.6D	0.25-0.35
					1D-2D
5	23	0.2D-1.0D	35°-55°	0.2D-1.0D	0.35-0.50
	24	0.2D-1.0D	35°-55°	0.2D-0.8D	0.35-0.50
	25	0.2D-1.0D	35°-55°	0.2D-0.6D	0.35-0.50
					1D-2D
	26	0.2D-1.0D	35°-55°	< 0.85R	0.05-0.15
10	27	0.2D-1.0D	35°-55°	< 0.85R	0.05-0.15
	28	0.2D-1.0D	35°-55°	< 0.85R	0.05-0.15
					1D-2D
	29	0.2D-1.0D	35°-55°	< 0.85R	0.15-0.25
	30	0.2D-1.0D	35°-55°	< 0.85R	0.15-0.25
15	31	0.2D-1.0D	35°-55°	< 0.85R	0.15-0.25
					1D-2D
	32	0.2D-1.0D	35°-55°	< 0.85R	0.25-0.35
	33	0.2D-1.0D	35°-55°	< 0.85R	0.25-0.35
	34	0.2D-1.0D	35°-55°	< 0.85R	0.25-0.35
20					1D-2D
	35	0.4D-0.6D	10°-35°	0 -0.6D	0.05-0.15
	36	0.4D-0.6D	10°-35°	0 -0.6D	0.05-0.15
	37	0.4D-0.6D	10°-35°	0 -0.6D	0.05-0.15
					1D-2D
25	38	0.4D-0.6D	10°-35°	0 -0.6D	0.15-0.25
	39	0.4D-0.6D	10°-35°	0 -0.6D	0.15-0.25
	40	0.4D-0.6D	10°-35°	0 -0.6D	0.15-0.25
					1D-2D
	41	0.4D-0.6D	10°-35°	0 -0.6D	0.25-0.35
30	42	0.4D-0.6D	10°-35°	0 -0.6D	0.25-0.35
	43	0.4D-0.6D	10°-35°	0 -0.6D	0.25-0.35
					1D-2D

- 10 -

	44	0.4D-0.6D	10°-35°	0 -0.6D	0.35-0.50	0	
	45	0.4D-0.6D	10°-35°	0 -0.6D	0.35-0.50	0-1D	
	46	0.4D-0.6D	10°-35°	0 -0.6D	0.35-0.50	1D-2D	
	5	47	0.4D-0.6D	10°-35°	0.6D-1D	0.05-0.15	0
		48	0.4D-0.6D	10°-35°	0.6D-0.8D	0.05-0.15	0-1D
		49	0.4D-0.6D	10°-35°	0.6D-1D	0.15-0.25	0
		50	0.4D-0.6D	10°-35°	0.6D-0.8D	0.15-0.25	0-1D
10		51	0.4D-0.6D	10°-35°	0.6D-1D	0.25-0.35	0
		52	0.4D-0.6D	10°-35°	0.6D-0.8D	0.25-0.35	0-1D
		53	0.4D-0.6D	10°-35°	0.6D-1D	0.35-0.50	0
15	54	0.4D-0.6D	10°-35°	0.6D-0.8D	0.35-0.50	0-1D	
		55	0.6D-1D	10°-35°	0 -0.6D	0.05-0.15	0
		56	0.6D-1D	10°-35°	0 -0.6D	0.05-0.15	0-1D
		57	0.6D-1D	10°-35°	0 -0.6D	0.05-0.15	1D-2D
20		58	0.6D-1D	10°-35°	0 -0.6D	0.15-0.25	0
		59	0.6D-1D	10°-35°	0 -0.6D	0.15-0.25	0-1D
		60	0.6D-1D	10°-35°	0 -0.6D	0.15-0.25	1D-2D
	25	61	0.6D-1D	10°-35°	0 -0.6D	0.25-0.35	0
		62	0.6D-1D	10°-35°	0 -0.6D	0.25-0.35	0-1D
		63	0.6D-1D	10°-35°	0 -0.6D	0.25-0.35	1D-2D
		64	0.6D-1D	10°-35°	0 -0.6D	0.35-0.50	0
30		65	0.6D-1D	10°-35°	0 -0.6D	0.35-0.50	0-1D
		66	0.6D-1D	10°-35°	0 -0.6D	0.35-0.50	1D-2D

- 11 -

67	0.6D-1D	10°-35°	0.6D-1D	0.05-0.15	0
68	0.6D-1D	10°-35°	0.6D-0.8D	0.05-0.15	0-1D
	69	0.6D-1D	10°-35°	0.6D-1D	0.15-0.25
5	70	0.6D-1D	10°-35°	0.6D-0.8D	0.15-0.25
	71	0.6D-1D	10°-35°	0.6D-1D	0.25-0.35
	72	0.6D-1D	10°-35°	0.6D-0.8D	0.25-0.35
10	73	0.6D-1D	10°-35°	0.6D-1D	0.35-0.50
	74	0.6D-1D	10°-35°	0.6D-0.8D	0.35-0.50
	75	0.4D-0.6D	10°-35°	< 0.85R	0.05-0.15
	76	0.4D-0.6D	10°-35°	< 0.85R	0.05-0.15
15	77	0.4D-0.6D	10°-35°	< 0.85R	0.05-0.15
	78	0.4D-0.6D	10°-35°	< 0.85R	0.15-0.25
	79	0.4D-0.6D	10°-35°	< 0.85R	0.15-0.25
	80	0.4D-0.6D	10°-35°	< 0.85R	0.15-0.25
20					1D-2D
	81	0.4D-0.6D	10°-35°	< 0.85R	0.25-0.35
	82	0.4D-0.6D	10°-35°	< 0.85R	0.25-0.35
	83	0.4D-0.6D	10°-35°	< 0.85R	0.25-0.35
25	84	0.4D-0.6D	10°-35°	< 0.85R	0.35-0.50
	85	0.4D-0.6D	10°-35°	< 0.85R	0.35-0.50
	86	0.4D-0.6D	10°-35°	< 0.85R	0.35-0.50
	87	0.6D-1D	10°-35°	< 0.85R	0.05-0.15
30	88	0.6D-1D	10°-35°	< 0.85R	0.05-0.15
	89	0.6D-1D	10°-35°	< 0.85R	0.05-0.15
					1D-2D

- 12 -

90	0.6D-1D	10°-35°	< 0.85R	0.15-0.25	0
91	0.6D-1D	10°-35°	< 0.85R	0.15-0.25	0-1D
	92	0.6D-1D	10°-35°	< 0.85R	0.15-0.25
					1D-2D
5	93	0.6D-1D	10°-35°	< 0.85R	0.25-0.35
	94	0.6D-1D	10°-35°	< 0.85R	0.25-0.35
	95	0.6D-1D	10°-35°	< 0.85R	0.25-0.35
					1D-2D
	96	0.6D-1D	10°-35°	< 0.85R	0.35-0.50
10	97	0.6D-1D	10°-35°	< 0.85R	0.35-0.50
	98	0.6D-1D	10°-35°	< 0.85R	0.35-0.50
					1D-2D

In preferred embodiments the distance between adjacent threads is smaller than 3D, preferably smaller than 2D.

15 In a further preferred embodiment the threads or macroroughness is combined with a microroughness having a pore size of 2 μ to 20 μ , preferably 2 μ to 10 μ . By such a combination of macroscopic and microscopic interlocking also implant surfaces which, if smooth, would not have interacted mechanically with the bone will take part in the transmission of the loads to
20 the bone. This will further tend to smooth away the stress concentrations which inevitably will arise in the bone tissue due to the macroscopic interlocking and which the invention is to alleviate, thus further enhancing the effect the invention is intended to achieve. The microscopic roughness may for instance be made by blasting or chemical etching, but is preferably made
25 by blasting with particles of TiO_2 .

Table 1: Thread depth = 0.1 mm. No straight part at the bottom of the thread. The value of σ_{\max}^+ for different combinations of flank angle and top radius as a result of a standard load per unit length of the implant segment. In the cases when $\sigma_{\max}^+/1.45$, $\sigma_{\max}^+/2.61$, $\sigma_{\max}^+/1.45$ or $\sigma_{\max}^+/2.61$ exceed σ_{\max}^+ these values are also given. The value of the top radius expressed as a coefficient multiplied with the thread depth (D).

Flank angle	T o p r a d i u s						D mm
	0.1xD mm	0.2xD mm	0.4xD mm	0.6xD mm	0.8xD mm		
0°	σ_{\max}^+	2.76	2.80	2.87	2.64	2.57	
	$\sigma_{\max}^+/1.45$				2.66	2.65	
	$\sigma_{\max}^+/1.45$					2.58	
10°	σ_{\max}^+	3.02	2.86	2.84	2.72	2.65	2.62
	$\sigma_{\max}^+/1.45$					2.81	3.10
	$\sigma_{\max}^+/1.45$						2.65
20°	σ_{\max}^+	2.78	2.55	2.52	2.64	2.63	2.51
	$\sigma_{\max}^+/1.45$					3.14	3.75
	$\sigma_{\max}^+/1.45$						2.90
30°	σ_{\max}^+	2.46	2.25	2.15	2.21	2.29	2.37
	$\sigma_{\max}^+/1.45$			2.22	2.72		3.29
	$\sigma_{\max}^+/1.45$						2.57
40°	σ_{\max}^+	2.17		1.98	1.83	1.81	1.89
	$\sigma_{\max}^+/1.45$	2.19		2.19	2.25	2.31	2.68
	$\sigma_{\max}^+/1.45$	2.25				1.91	2.00
50°	σ_{\max}^+	2.15		1.88	1.67	1.59	1.56
	$\sigma_{\max}^+/1.45$	2.70		2.53	2.52	2.55	2.66
	$\sigma_{\max}^+/1.45$	2.51		2.27	2.03	1.95	2.01
60°	σ_{\max}^+	2.49	2.22	1.89	1.71	1.61	1.55
	$\sigma_{\max}^+/1.45$	3.68	3.53	3.31	3.13	3.30	3.48
	$\sigma_{\max}^+/2.61$					1.74	1.83
	$\sigma_{\max}^+/1.45$	3.10	2.90	2.66	2.46	2.43	2.56

Table 2: Thread depth = 0.2 mm. No straight part at the bottom of the thread. The value of σ_{\max}^+ for different combinations of flank angle and top radius as a result of a standard load per unit length of the implant segment. In the cases when $\sigma_{\max}^+ / 1.45$, $\sigma_{\max}^+ / 2.61$, $\sigma_{\max}^+ / 1.45$ or $\sigma_{\max}^+ / 2.61$ exceed σ_{\max}^+ these values are also given. The value of the top radius expressed as a coefficient multiplied with the thread depth (D).

Flank angle	T o p r a d i u s						D mm
	0.1xD mm	0.2xD mm	0.4xD mm	0.6xD mm	0.8xD mm		
0°	σ_{\max}^+	2.65	2.59	2.44	2.24	2.19	
	$\sigma_{\max}^+ / 1.45$				2.30	2.36	
	$\sigma_{\max}^+ / 1.45$					2.28	
10°	σ_{\max}^+	2.96	2.62	2.39	2.25	2.08	2.12
	$\sigma_{\max}^+ / 1.45$					2.27	2.40
	$\sigma_{\max}^+ / 1.45$					2.17	2.32
20°	σ_{\max}^+	2.80	2.51	2.34	2.23	2.06	1.99
	$\sigma_{\max}^+ / 1.45$					2.63	3.11
	$\sigma_{\max}^+ / 1.45$					2.10	2.46
30°	σ_{\max}^+	2.51	2.28	2.12	2.06	2.01	1.98
	$\sigma_{\max}^+ / 1.45$					2.37	2.84
	$\sigma_{\max}^+ / 1.45$						2.26
40°	σ_{\max}^+	2.23	2.02	1.86	1.81	1.78	1.78
	$\sigma_{\max}^+ / 1.45$	2.63	2.32	2.08	2.09	2.12	2.41
	$\sigma_{\max}^+ / 1.45$	2.37					1.93
50°	σ_{\max}^+	2.24	1.95	1.72	1.63	1.59	1.57
	$\sigma_{\max}^+ / 1.45$	3.14	3.18	2.52	2.38	2.39	2.42
	$\sigma_{\max}^+ / 1.45$	2.68	2.37	2.01	1.96	1.90	1.92
60°	σ_{\max}^+	2.58	2.30	1.94	1.76	1.66	1.59
	$\sigma_{\max}^+ / 1.45$	4.09	3.83	3.50	3.10	3.41	3.60
	$\sigma_{\max}^+ / 2.61$			1.95	1.82	1.90	2.00
	$\sigma_{\max}^+ / 1.45$	3.38	3.10	2.69	2.43	2.54	2.67

Table 3: Thread depth = 0.3 mm. No straight part at the bottom of the thread. The value of σ_{\max}^+ for different combinations of flank angle and top radius as a result of a standard load per unit length of the implant segment. In the cases when $\sigma_{\max}^+/1.45$, $\sigma_{\max}^+/2.61$, $\sigma_{e,\max}^+/1.45$ or $\sigma_{e,\max}^+/2.61$ exceed σ_{\max}^+ these values are also given. The value of the top radius expressed as a coefficient multiplied with the thread depth (D).

Flank angle	T o p r a d i u s					
	0.1xD mm	0.2xD mm	0.4xD mm	0.6xD mm	0.8xDmm	D mm
0°	σ_{\max}^+	2.54	2.42	2.11	2.04	1.99
	$\sigma_{\max}^+/1.45$				2.17	2.21
	$\sigma_{\max}^+/1.45$				2.14	2.19
10°	σ_{\max}^+	2.82	2.43	2.13	1.92	1.88
	$\sigma_{\max}^+/1.45$				2.12	2.23
	$\sigma_{\max}^+/1.45$				2.08	2.20
20°	σ_{\max}^+	2.78	2.42	2.12	1.95	1.80
	$\sigma_{\max}^+/1.45$				1.98	2.44
	$\sigma_{\max}^+/1.45$				1.97	2.88
30°	σ_{\max}^+	2.54	2.27	2.04	1.91	1.78
	$\sigma_{\max}^+/1.45$				2.23	2.26
	$\sigma_{\max}^+/1.45$				1.88	2.16
40°	σ_{\max}^+	2.29		2.04	1.86	1.77
	$\sigma_{\max}^+/1.45$	2.73		2.37	1.97	1.97
	$\sigma_{\max}^+/1.45$	2.39				2.01
50°	σ_{\max}^+	2.30	1.99		1.75	1.65
	$\sigma_{\max}^+/1.45$	3.25	2.94		2.54	2.29
	$\sigma_{\max}^+/1.45$	2.77	2.37		2.01	1.92
60°	σ_{\max}^+	2.64	2.34	1.98	1.80	1.69
	$\sigma_{\max}^+/1.45$	4.18	3.90	3.54	3.38	3.57
	$\sigma_{\max}^+/2.61$				1.88	1.98
	$\sigma_{\max}^+/1.45$	3.48	3.16	2.68	2.56	2.68

Table 4: Thread depth = 0.4 mm. No straight part at the bottom of the thread. The value of σ_{\max}^+ for different combinations of flank angle and top radius as a result of a standard load per unit length of the implant segment. In the cases when $\sigma_{\max}^+/1.45$, $\sigma_{\max}^+/2.61$, $\sigma_{\max}/1.45$ or $\sigma_{\max}/2.61$ exceed σ_{\max}^+ these values are also given. The value of the top radius expressed as a coefficient multiplied with the thread depth (D).

Flank angle	T o p r a d i u s						D mm
	0.1xD mm	0.2xD mm	0.4xD mm	0.6xD mm	0.8xDmm		
0°	σ_{\max}^+	2.41	2.22	1.96	1.91	1.87	
	$\sigma_{\max}^+/1.45$			2.07	2.11		
	$\sigma_{\max}^+/1.45$			2.08	2.14		
10°	σ_{\max}^+	2.72	2.26	1.93	1.75	1.77	1.81
	$\sigma_{\max}^+/1.45$			1.82	2.01	2.14	
	$\sigma_{\max}^+/1.45$			1.87	2.04	2.16	
20°	σ_{\max}^+	2.76	2.34	1.96	1.75	1.62	1.58
	$\sigma_{\max}^+/1.45$			1.90	2.35	2.77	
	$\sigma_{\max}^+/1.45$				1.92	2.23	
30°	σ_{\max}^+	2.55	2.26	1.96	1.75	1.63	1.52
	$\sigma_{\max}^+/1.45$			1.78	2.15	2.58	
	$\sigma_{\max}^+/1.45$				1.84	2.12	
40°	σ_{\max}^+	2.33	2.06	1.85	1.72	1.60	1.52
	$\sigma_{\max}^+/1.45$	2.77	2.38	1.94	1.90	1.95	2.22
	$\sigma_{\max}^+/1.45$	2.39				1.66	1.84
50°	σ_{\max}^+	2.35	2.03	1.76	1.65	1.58	1.51
	$\sigma_{\max}^+/1.45$	3.29	2.95	2.54	2.27	2.23	2.43
	$\sigma_{\max}^+/1.45$	2.81	2.35	2.01	1.90	1.81	1.94
60°	σ_{\max}^+	2.68	2.38	2.01	1.82	1.70	1.63
	$\sigma_{\max}^+/1.45$	4.21	3.92	3.53	3.54	3.74	3.93
	$\sigma_{\max}^+/2.61$				1.97	2.08	2.18
	$\sigma_{\max}^+/1.45$	3.59	3.20	2.68	2.70	2.83	2.97
	$\sigma_{\max}^+/2.61$						1.65

Table 5: Thread depth = 0.1 mm. The lengths of the straight part of S at the bottom of the thread which minimize the maximum compressive stress, the maximum tensile stress and the maximum von Mises stress respectively. This length is expressed as a coefficient c which is to be multiplied with the length of the curved part (L) of the thread (Fig. 1). The table lists the values of this coefficient.

Flank angle	Min. Stress	T o p r a d i u s					
		0.1xD mm	0.2xD mm	0.4xD mm	0.6xD mm	0.8xDmm	1xD mm
0°	$\sigma_{\text{c,max}}$	0	0.4	0.2	0.2	0.2	-
	$\sigma_{\text{t,max}}$	0	0.4	0.4	0.8	0.8	-
	σ_{vmax}	0	0.4	0.4	0.4	0.2	-
10°	$\sigma_{\text{c,max}}$	0	0	0	0	0	0
	$\sigma_{\text{t,max}}$	0	0	0.8	0.8	0.8	0.8
	σ_{vmax}	0	0	0.4	0.4	0.2	0
20°	$\sigma_{\text{c,max}}$	0	0	0	0.2	0.2	0
	$\sigma_{\text{t,max}}$	0	0	0.4	0.8	0.8	0.4
	σ_{vmax}	0	0	0.4	0.4	0.4	0.2
30°	$\sigma_{\text{c,max}}$	0	0	0	0	0	0
	$\sigma_{\text{t,max}}$	0	0	0	0.4	0.4	0.4
	σ_{vmax}	0	0	0	0.2	0.2	0.2
40°	$\sigma_{\text{c,max}}$	0	0	0	0	0	0
	$\sigma_{\text{t,max}}$	0	0	0	0.2	0.2	0.2
	σ_{vmax}	0	0	0	0	0	0.2
50°	$\sigma_{\text{c,max}}$	0	0	0	0	0	0
	$\sigma_{\text{t,max}}$	0	0	0	0	0	0
	σ_{vmax}	0	0	0	0	0	0
60°	$\sigma_{\text{c,max}}$	0	0	0	0	0	0
	$\sigma_{\text{t,max}}$	0	0	0	0	0	0
	σ_{vmax}	0	0	0	0	0	0

Table 6: Thread depth = 0.2 mm. The lengths of the straight part of S at the bottom of the thread which minimize the maximum compressive stress, the maximum tensile stress and the maximum von Mises stress respectively. This length is expressed as a coefficient c which is to be multiplied with the length of the curved part (L) of the thread (Fig. 1). The table lists the values of this coefficient.

Flank angle	Min. Stress	T o p r a d i u s					
		0.1xD mm	0.2xD mm	0.4xD mm	0.6xD mm	0.8xDmm	1xD mm
0°	σ_{max}	0	0.4	0.4	0.2	0	-
	$\sigma_{\text{+max}}$	0	0.4	0.4	0.8	0.8	-
	$\sigma_{\text{e,max}}$	0	0.4	0.4	0.8	0.2	-
10°	σ_{max}	0	0	0.2	0	0	0
	$\sigma_{\text{+max}}$	0	0.2	0.4	0.8	0.8	0.8
	$\sigma_{\text{e,max}}$	0	0	0.4	0.4	0.2	0
20°	σ_{max}	0	0	0	0	0	0
	$\sigma_{\text{+max}}$	0	0	0.4	0.8	0.4	0.8
	$\sigma_{\text{e,max}}$	0	0	0.2	0.4	0.4	0.2
30°	σ_{max}	0	0	0	0	0	0
	$\sigma_{\text{+max}}$	0	0	0	0.4	0.4	0.4
	$\sigma_{\text{e,max}}$	0	0	0	0.2	0.2	0.2
40°	σ_{max}	0	0	0	0	0	0
	$\sigma_{\text{+max}}$	0	0	0	0	0.2	0.2
	$\sigma_{\text{e,max}}$	0	0	0	0	0	0.2
50°	σ_{max}	0	0	0	0	0	0
	$\sigma_{\text{+max}}$	0	0	0	0	0	0
	$\sigma_{\text{e,max}}$	0	0	0	0	0	0
60°	σ_{max}	0	0	0	0	0	0
	$\sigma_{\text{+max}}$	0	0	0	0	0	0
	$\sigma_{\text{e,max}}$	0	0	0	0	0	0

Table 7: Thread depth = 0.3 mm. The lengths of the straight part of S at the bottom of the thread which minimize the maximum compressive stress, the maximum tensile stress and the maximum von Mises stress respectively. This length is expressed as a coefficient c which is to be multiplied with the length of the curved part (L) of the thread (Fig. 1). The table lists the values of this coefficient.

Flank angle	Min. Stress	T o p r a d i u s					
		0.1xD mm	0.2xD mm	0.4xD mm	0.6xD mm	0.8xDmm	1xD mm
0°	$\sigma_{\text{c,max}}$	0	0.4	0.4	0.2	0	-
	$\sigma_{\text{t,max}}$	0.2	0.4	0.8	0.8	0.8	-
	$\sigma_{\text{vM,max}}$	0	0.4	0.4	0.8	0.2	-
10°	$\sigma_{\text{c,max}}$	0	0	0.2	0	0	0
	$\sigma_{\text{t,max}}$	0	0	0.4	0.8	0.8	0.4
	$\sigma_{\text{vM,max}}$	0	0	0.4	0.4	0.2	0
20°	$\sigma_{\text{c,max}}$	0	0	0	0	0	0
	$\sigma_{\text{t,max}}$	0	0	0.2	0.4	0.4	0.4
	$\sigma_{\text{vM,max}}$	0	0	0.2	0.4	0.2	0.2
30°	$\sigma_{\text{c,max}}$	0	0	0	0	0	0
	$\sigma_{\text{t,max}}$	0	0	0	0.4	0.2	0.4
	$\sigma_{\text{vM,max}}$	0	0	0	0.2	0.2	0.2
40°	$\sigma_{\text{c,max}}$	0	0	0	0	0	0
	$\sigma_{\text{t,max}}$	0	0	0	0	0	0.2
	$\sigma_{\text{vM,max}}$	0	0	0	0	0	0
50°	$\sigma_{\text{c,max}}$	0	0	0	0	0	0
	$\sigma_{\text{t,max}}$	0	0	0	0	0	0
	$\sigma_{\text{vM,max}}$	0	0	0	0	0	0
60°	$\sigma_{\text{c,max}}$	0	0	0	0	0	0
	$\sigma_{\text{t,max}}$	0	0	0	0	0	0
	$\sigma_{\text{vM,max}}$	0	0	0	0	0	0

Table 8: Thread depth = 0.4 mm. The lengths of the straight part of S at the bottom of the thread which minimize the maximum compressive stress, the maximum tensile stress and the maximum von Mises stress respectively. This length is expressed as a coefficient c which is to be multiplied with the length of the curved part (L) of the thread (Fig. 1). The table lists the values of this coefficient.

Flank angle	Min. Stress	T o p r a d i u s					
		0.1xD mm	0.2xD mm	0.4xD mm	0.6xD mm	0.8xDmm	1xD mm
0°	σ'_{\max}	0	0.4	0.4	0.2	0	-
	σ^+_{\max}	0	0.4	0.4	0.8	0.8	-
	$\sigma_{\epsilon,\max}$	0	0.2	0.4	0.8	0.2	-
10°	σ'_{\max}	0	0	0.2	0	0	0
	σ^+_{\max}	0	0	0.2	0.4	0.8	0.8
	$\sigma_{\epsilon,\max}$	0	0	0.2	0.4	0.2	0
20°	σ'_{\max}	0	0	0	0	0	0
	σ^+_{\max}	0	0	0	0.2	0.4	0.4
	$\sigma_{\epsilon,\max}$	0	0	0	0.2	0.2	0.2
30°	σ'_{\max}	0	0	0	0	0	0
	σ^+_{\max}	0	0	0	0	0.2	0.2
	$\sigma_{\epsilon,\max}$	0	0	0	0.2	0.2	0
40°	σ'_{\max}	0	0	0	0	0	0
	σ^+_{\max}	0	0	0	0	0	0
	$\sigma_{\epsilon,\max}$	0	0	0	0	0	0
50°	σ'_{\max}	0	0	0	0	0	0
	σ^+_{\max}	0	0	0	0	0	0
	$\sigma_{\epsilon,\max}$	0	0	0	0	0	0
60°	σ'_{\max}	0	0	0	0	0	0
	σ^+_{\max}	0	0	0	0	0	0
	$\sigma_{\epsilon,\max}$	0	0	0	0	0	0

Table 9: Thread depth = 0.1 mm. The lowest of the values of σ_{\max}^+ for different lengths of the straight part at the bottom of the thread ($c = 0, 0.2, 0.4, 0.8, 1.6$) for different combinations of flank angle and top radius as a result of a standard load per unit length of the implant segment. In the cases when $\sigma_{\max}^+ / 1.45, \sigma_{\max}^+ / 2.61, \sigma_{\max}^+ / 1.45$ or $\sigma_{\max}^+ / 2.61$ exceed σ_{\max}^+ these values are also given (for the combination of parameters which minimized σ_{\max}^+). The value of the top radius expressed as a coefficient multiplied with the thread depth (D).

Flank angle	T o p r a d i u s						D mm
	0.1xD mm	0.2xD mm	0.4xD mm	0.6xD mm	0.8xD mm		
0°	σ_{\max}^+	2.76	2.48	2.33	2.13	2.02	
	$\sigma_{\max}^+ / 1.45$				2.92	6.17	
	$\sigma_{\max}^+ / 2.61$					3.42	
	$\sigma_{\max}^+ / 1.45$					3.48	
10°	σ_{\max}^+	3.02	2.86	2.54	2.32	2.11	2.05
	$\sigma_{\max}^+ / 1.45$				3.05	4.59	8.71
	$\sigma_{\max}^+ / 2.61$					2.55	4.84
	$\sigma_{\max}^+ / 1.45$					2.66	5.24
	$\sigma_{\max}^+ / 2.61$						2.91
20°	σ_{\max}^+	2.78	2.55	2.46	2.27	2.18	2.06
	$\sigma_{\max}^+ / 1.45$				3.02	4.04	4.23
	$\sigma_{\max}^+ / 2.61$					2.25	2.35
	$\sigma_{\max}^+ / 1.45$					2.44	2.64
30°	σ_{\max}^+	2.46	2.25	2.15	2.05	2.01	1.97
	$\sigma_{\max}^+ / 1.45$				2.46	2.95	3.58
	$\sigma_{\max}^+ / 2.61$						1.99
	$\sigma_{\max}^+ / 1.45$					2.10	2.34
40°	σ_{\max}^+	2.17			1.98	1.83	1.80
	$\sigma_{\max}^+ / 1.45$	2.19		2.25		2.52	2.58
	$\sigma_{\max}^+ / 1.45$	2.24			1.99	2.02	2.11
50°	σ_{\max}^+	2.15		1.88	1.67	1.59	1.56
	$\sigma_{\max}^+ / 1.45$	2.70		2.53	2.52	2.55	2.60
	$\sigma_{\max}^+ / 1.45$	2.51		2.27	2.03	1.95	2.02
60°	σ_{\max}^+	2.49	2.22	1.89	1.71	1.61	1.55
	$\sigma_{\max}^+ / 1.45$	3.68	3.53	3.31	3.13	3.30	3.48
	$\sigma_{\max}^+ / 2.61$				1.74	1.83	1.93
	$\sigma_{\max}^+ / 1.45$	3.11	2.91	2.66	2.46	2.43	2.56

Table 10: Thread depth = 0.2 mm. The lowest of the values of σ_{\max}^+ for different lengths of the straight part at the bottom of the thread ($c = 0, 0.2, 0.4, 0.8, 1.6$) for different combinations of flank angle and top radius as a result of a standard load per unit length of the implant segment. In the cases when $\sigma_{\max}^+/1.45$, $\sigma_{\max}^+/2.61$, $\sigma_{\max}/1.45$ or $\sigma_{\max}/2.61$ exceed σ_{\max}^+ these values are also given (for the combination of parameters which minimized σ_{\max}^+). The value of the top radius expressed as a coefficient multiplied with the thread depth (D).

Flank angle		T o p r a d i u s					
		0.1xD mm	0.2xD mm	0.4xD mm	0.6xD mm	0.8xD mm	D mm
0°	σ_{\max}^+	2.65	2.35	2.11	1.89	1.74	
	$\sigma_{\max}/1.45$				2.62	5.59	
	$\sigma_{\max}/2.61$					3.10	
	$\sigma_{\max}/1.45$					3.18	
	$\sigma_{\max}/2.61$					1.77	
10°	σ_{\max}^+	2.96	2.61	2.25	1.97	1.85	1.71
	$\sigma_{\max}/1.45$				2.72	4.12	7.86
	$\sigma_{\max}/2.61$					2.29	4.37
	$\sigma_{\max}/1.45$					2.44	4.75
	$\sigma_{\max}/2.61$						2.64
20°	σ_{\max}^+	2.80	2.51	2.28	2.08	1.93	1.78
	$\sigma_{\max}/1.45$				2.23	2.83	3.72
	$\sigma_{\max}/2.61$						2.07
	$\sigma_{\max}/1.45$						2.39
30°	σ_{\max}^+	2.51	2.28	2.12	2.01	1.88	1.79
	$\sigma_{\max}/1.45$				2.20	2.63	3.19
	$\sigma_{\max}/1.45$					1.89	2.12
40°	σ_{\max}^+	2.24	2.02	1.86	1.81	1.77	1.71
	$\sigma_{\max}/1.45$	2.63	2.32	2.08	2.09	2.30	2.56
	$\sigma_{\max}/1.45$	2.37				1.81	1.92
50°	σ_{\max}^+	2.24	1.95	1.72	1.63	1.59	1.57
	$\sigma_{\max}/1.45$	3.14	2.87	2.52	2.38	2.39	2.42
	$\sigma_{\max}/1.45$	2.67	2.37	2.01	1.96	1.90	1.92
60°	σ_{\max}^+	2.58	2.30	1.94	1.76	1.66	1.59
	$\sigma_{\max}/1.45$	4.09	3.83	3.50	3.28	3.41	3.60
	$\sigma_{\max}/2.61$	2.27	2.13	1.95	1.82	1.90	2.00
	$\sigma_{\max}/1.45$	3.38	3.10	2.69	2.43	2.54	2.67

Table 11: Thread depth = 0.3 mm. The lowest of the values of σ_{\max}^+ for different lengths of the straight part at the bottom of the thread ($c = 0, 0.2, 0.4, 0.8, 1.6$) for different combinations of flank angle and top radius as a result of a standard load per unit length of the implant segment. In the cases when $\sigma_{\max}/1.45$, $\sigma_{\max}/2.61$, $\sigma_{\max}/1.45$ or $\sigma_{\max}/2.61$ exceed σ_{\max}^+ these values are also given (for the combination of parameters which minimized σ_{\max}^+). The value of the top radius expressed as a coefficient multiplied with the thread depth (D).

Flank angle	T o p r a d i u s						D mm
	0.1xD mm	0.2xD mm	0.4xD mm	0.6xD mm	0.8xD mm		
0°	σ_{\max}^+	2.48	2.20	1.93	1.72	1.59	
	$\sigma_{\max}/1.45$			2.50	5.38		
	$\sigma_{\max}/2.61$				2.98		
	$\sigma_{\max}/1.45$				3.07		
	$\sigma_{\max}/2.61$				1.70		
10°	σ_{\max}^+	2.82	2.43	2.04	1.81	1.63	1.54
	$\sigma_{\max}/1.45$			2.12	3.97		7.62
	$\sigma_{\max}/2.61$				2.20		4.23
	$\sigma_{\max}/1.45$				2.38		4.62
	$\sigma_{\max}/2.61$						2.57
20°	σ_{\max}^+	2.77	2.42	2.11	1.88	1.68	1.57
	$\sigma_{\max}/1.45$			2.11	2.70		3.55
	$\sigma_{\max}/2.61$				1.97		
	$\sigma_{\max}/1.45$				1.88		2.32
	$\sigma_{\max}/1.45$						
30°	σ_{\max}^+	2.53	2.27	2.04	1.91	1.72	1.60
	$\sigma_{\max}/1.45$				2.30		3.05
	$\sigma_{\max}/2.61$						1.69
	$\sigma_{\max}/1.45$				1.79		2.08
	$\sigma_{\max}/1.45$						
40°	σ_{\max}^+	2.29	2.04	1.86	1.77	1.70	1.63
	$\sigma_{\max}/1.45$	2.73	2.37	1.97	1.97	2.01	2.61
	$\sigma_{\max}/1.45$	2.39					1.88
	$\sigma_{\max}/1.45$						
	$\sigma_{\max}/1.45$						
50°	σ_{\max}^+	2.30	2.00	1.75	1.65	1.59	1.55
	$\sigma_{\max}/1.45$	3.25	2.94	2.54	2.29	2.28	2.34
	$\sigma_{\max}/1.45$	2.77	2.36	2.01	1.92	1.83	1.85
	$\sigma_{\max}/1.45$						
	$\sigma_{\max}/1.45$						
60°	σ_{\max}^+	2.64	2.34	1.98	1.80	1.69	1.62
	$\sigma_{\max}/1.45$	4.18	3.90	3.54	3.38	3.56	3.75
	$\sigma_{\max}/2.61$				1.88	1.98	2.08
	$\sigma_{\max}/1.45$	3.48	3.16	2.68	2.56	2.68	2.81
	$\sigma_{\max}/1.45$						

Table 12: Thread depth = 0.4 mm. The lowest of the values of σ_{\max}^+ for different lengths of the straight part at the bottom of the thread ($c = 0, 0.2, 0.4, 0.8, 1.6$) for different combinations of flank angle and top radius as a result of a standard load per unit length of the implant segment. In the cases when $\sigma_{\max}^+ / 1.45$, $\sigma_{\max}^+ / 2.61$, $\sigma_{\max}^+ / 1.45$ or $\sigma_{\max}^+ / 2.61$ exceed σ_{\max}^+ these values are also given (for the combination of parameters which minimized σ_{\max}^+). The value of the top radius expressed as a coefficient multiplied with the thread depth (D).

Flank angle	Top radius					
	0.1xD mm	0.2xD mm	0.4xD mm	0.6xD mm	0.8xD mm	D mm
0°	σ_{\max}^+	2.41	2.08	1.79	1.65	1.53
	$\sigma_{\max}^+ / 1.45$			2.46		5.31
	$\sigma_{\max}^+ / 2.61$				2.95	
	$\sigma_{\max}^+ / 1.45$			1.75		3.03
	$\sigma_{\max}^+ / 2.61$					1.69
10°	σ_{\max}^+	2.72	2.26	1.88	1.67	1.52
	$\sigma_{\max}^+ / 1.45$			2.06		3.92
	$\sigma_{\max}^+ / 2.61$				2.18	2.77
	$\sigma_{\max}^+ / 1.45$				2.39	4.59
	$\sigma_{\max}^+ / 2.61$					2.55
20°	σ_{\max}^+	2.76	2.34	1.96	1.72	1.55
	$\sigma_{\max}^+ / 1.45$			1.94		2.64
	$\sigma_{\max}^+ / 2.61$				1.94	3.49
	$\sigma_{\max}^+ / 1.45$				1.87	2.32
30°	σ_{\max}^+	2.55	2.26	1.96	1.75	1.59
	$\sigma_{\max}^+ / 1.45$			1.78		2.24
	$\sigma_{\max}^+ / 2.61$				1.78	1.50
	$\sigma_{\max}^+ / 1.45$					1.99
40°	σ_{\max}^+	2.33	2.06	1.85	1.72	1.60
	$\sigma_{\max}^+ / 1.45$	2.76	2.38	1.94	1.90	1.95
	$\sigma_{\max}^+ / 1.45$	2.39			1.66	2.22
50°	σ_{\max}^+	2.34	2.03	1.76	1.65	1.58
	$\sigma_{\max}^+ / 1.45$	3.29	2.95	2.54	2.27	2.23
	$\sigma_{\max}^+ / 1.45$	2.81	2.35	2.01	1.90	1.81
60°	σ_{\max}^+	2.68	2.38	2.01	1.82	1.70
	$\sigma_{\max}^+ / 1.45$	4.21	3.92	3.53	3.54	3.74
	$\sigma_{\max}^+ / 2.61$				1.97	2.08
	$\sigma_{\max}^+ / 1.45$	3.59	3.20	2.69	2.70	2.83
	$\sigma_{\max}^+ / 2.61$					2.97
						1.65

The radius R has been constant and has been real in the above examples.

In a preferred embodiment, illustrated in Fig 7, the top radius R at 5 the apex is imaginary and defines a the transition point P1 between the straight flank and the curved apex, a first tangent through P1 being directed along said flank, as well as a crest point P2 on the apex in which a second tangent to the curved part is parallel to the longitudinal direction of the implant. In this embodiment the curved apex has the shape of 10 curved part originating in said points P1 and P2 and has tangents in said points coinciding with said first and second tangents, and has a radius of curvature R1. The radius R1 may for instance increase from a value R_{\min} to a value R_{\max} or may increase from a value R_{\min} to a value R_{\max} , then decreasing to a value R_{\min} .

15 R_{\min} should preferably be greater than 0.01 mm and the relationship R_{\max}/R_{\min} preferably should be greater than 3.

One special case of this embodiment is of course that said radius of curvature R1 is constant and equal to said imaginary radius R, the apex thus having a part circular shape with the radius R.

20 The following calculations illustrate the effect of the variable radius of curvature.

Uniform top radius = 0.04 mm

Flank angle: 40°

Thread depth: 0.1mm

25 Bottom radius: 0.01mm

Maximum tensile stress: 1.784Mpa

Variable radius of curvature of the thread top-small continuous variations:

30 Flank angle: 40°

Thread depth: 0,1mm

Top radius: $R_{\min} = 0,025\text{mm}$, $R_{\max} = 0,055\text{mm}$

- 26 -

Bottom radius: 0.01mm

Maximum tensile stress: 1.750Mpa

Variable radius of curvature of the thread top - bigger continuous
5 variations:

Flank angle: 40°

Thread depth: 0,1mm

Top radius: $R_{min} = 0.0010\text{mm}$, $R_{max} = 0.069\text{mm}$

Bottom radius: 0.01mm

10 Maximum tensile stress: 1.721Mpa

As can be seen in the above, there is some improvement with a
variable radius of curvature.

The invention of course can be varied in many ways within the
15 scope of the appended claims. It should for instance be noted that the two
flank angles of the thread or roughness not necessarily have to be identical
even if this is a preferred embodiment. In some applications the angles may
be different although both are within the ranges specified, in another
applications it may be sufficient that the flank being the most heavily
20 loaded has a flank angle within the ranges specified. The same is valid for
the top radius which in similarity may have different values on the
respective sides of the thread, both values or only one value being within
the ranges specified.

CLAIMS

1. Thread or oriented macroroughness for bone implants,
5 particularly threaded dental implants, a section of said thread or roughness
(i.e. the profile) comprising two flanks and a curved apex, an imaginary top
radius R at the apex formed by the intersection of said two flanks defining
the transition point P1 between the straight flank and the curved apex, a
first tangent through P1 being directed along said flank, as well as a crest
10 point P2 on the apex in which a second tangent to the curved part is
parallel to the longitudinal direction of the implant, a curved part originating
in said points P1 and P2 and having tangents in said points coinciding with
said first and second tangents, forming said curved apex, having a radius
of curvature R1, a bottom length S, a bottom radius r formed at the bottom
15 of the groove between two adjacent threads or roughnesses, said flanks
forming an angle v with a plane which is perpendicular to the cross-section
of said thread or roughness and perpendicular to the surface of the implant
body, said profile further having a height D, **characterized** in that, for $10^\circ \leq v < 35^\circ$, R is greater than $0.4xD$ and that, for $35^\circ \leq v \leq 55^\circ$, R is
20 greater than $0.2xD$.
2. Thread or oriented macroroughness according to claim 1,
characterized in that for $0.15 \leq D \leq 0.25$ mm, $10^\circ \leq v < 35^\circ$ and $0.5D \leq S \leq 2D$, R is greater than $0.5D$ but smaller than $0.7D$.
3. Thread or oriented macroroughness according to claim 1,
25 **characterized** in that, for $0.05 \text{ mm} \leq D \leq 0.5 \text{ mm}$ and $35^\circ \leq v \leq 55^\circ$,
the top radius R is larger than $0.2xD$ but smaller than D, and in that, for
 $0.25 \text{ mm} \leq D \leq 0.5 \text{ mm}$ and $10^\circ \leq v < 35^\circ$, R is greater than $0.4xD$
but smaller than D.
4. Thread or oriented macroroughness according to claim 3,
30 **characterized** in that, for $0.25 \text{ mm} \leq D \leq 0.5 \text{ mm}$ and $10^\circ \leq v < 35^\circ$,
R is greater than $0.6xD$ but smaller than D.

5. Thread or oriented macroroughness according to claim 3,
characterized in that $0.05 \leq D \leq 0.25$ mm for $35^\circ \leq v \leq 55^\circ$.

6. Thread or oriented macroroughness according to claim 5,
characterized in that $0.05 \leq D \leq 0.15$ mm for $35^\circ \leq v \leq 55^\circ$.

7. Thread or oriented macroroughness according to claim 6,
characterized in that $0.05 \leq D \leq 0.1$ mm for $35^\circ \leq v \leq 55^\circ$.

8. Thread or oriented macroroughness according to claim 1
characterized in that $0.03 \leq R \leq 0.05$ mm, $37^\circ \leq v \leq 43^\circ$, $0.01 \leq r \leq 0.025$ and $0.08 \leq D \leq 0.15$.

10 9. Thread or oriented macroroughness according to any one of the
preceding claims **characterized in that** the distance between two adjacent
threads, crest to crest, is smaller than $3D$, preferably smaller than $2D$.

10 10. Thread or oriented macroroughness according to any one of the
preceding claims **characterized in that** said radius of curvature $R1$ is
15 constant and equal to said imaginary radius R .

11. Thread or oriented macroroughness according to any one of the
claims 1 - 9, **characterized in that** said radius of curvature $R1$ varies
between a minimum value R_{min} and a maximum value R_{max} .

12. Thread or oriented macroroughness according to claim 11,
20 **characterized in that** the relationship R_{max}/R_{min} is greater than 3.

13. Thread or oriented macroroughness according to claim 11 or
12, **characterized in that** R_{min} is greater than 0.01 mm.

14. Thread or oriented macroroughness according to any one of the
preceding claims **characterized in that** said thread profile is symmetric.

25 15. Thread or oriented macroroughness according to any one of
claims 1 - 13 **characterized in that** said radius R or $R1$ is located on one
first thread flank, the second thread flank being provided with another
radius at the apex of the thread which may be different from said first
radius or not and which has one tangent coinciding with said second flank
30 and one tangent through $P2$ which is parallel with the longitudinal axis of
the implant.

- 29 -

16. Thread or oriented macroroughness according to any one of the preceding claims, **characterized** in that said threads or macroroughness is combined with a superimposed microroughness having a pore size of 2μ to 20μ , preferably 2μ to 10μ .

17. Implant **characterized** in that said implant at least partly is provided with threads or oriented macroroughness according to any one of the preceding claims.

18. Implant according to claim 11, **characterized** in that said implant is provided with at least one additional, different thread.

WO 97/29713

PCT/SE97/00212

1/6

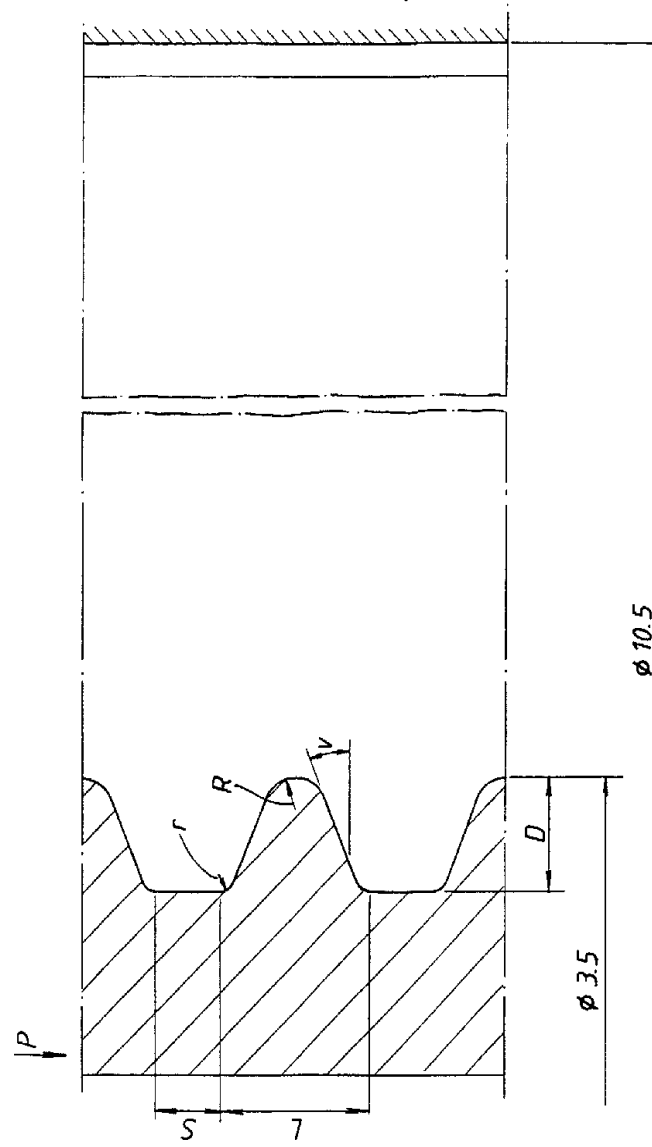


Fig.1

2/6

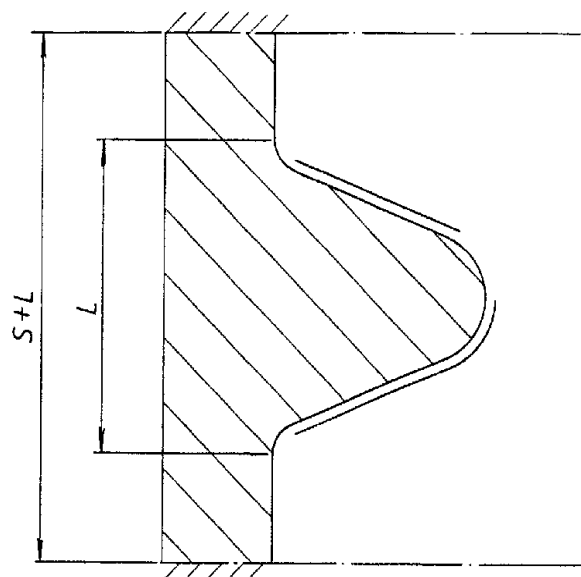


Fig.2

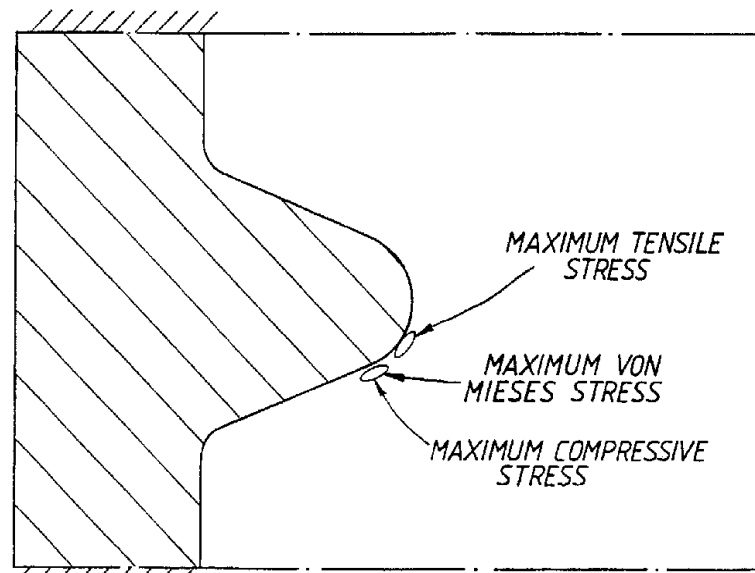


Fig.6

3/6

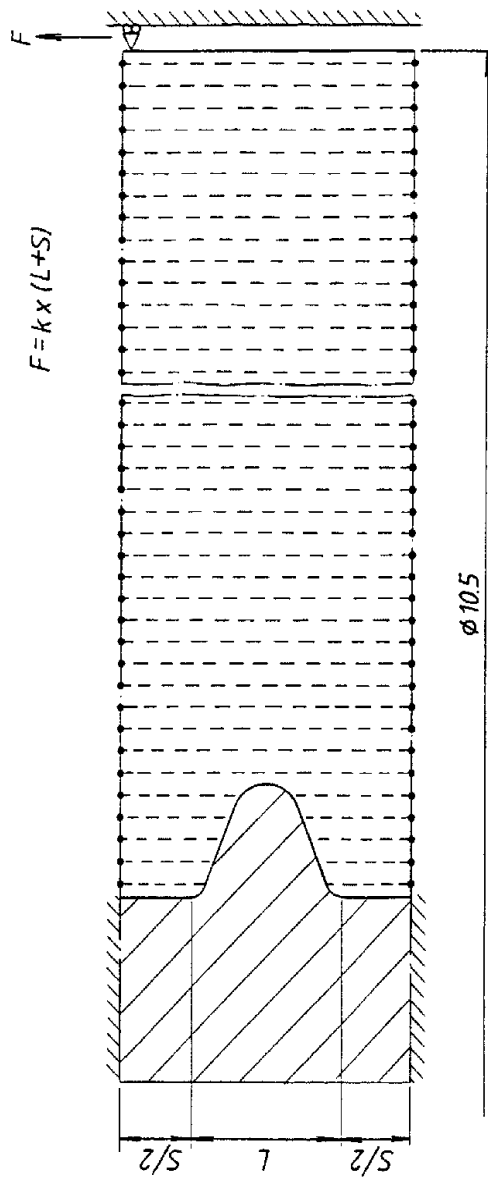


Fig.3

WO 97/29713

PCT/SE97/00212

4/6

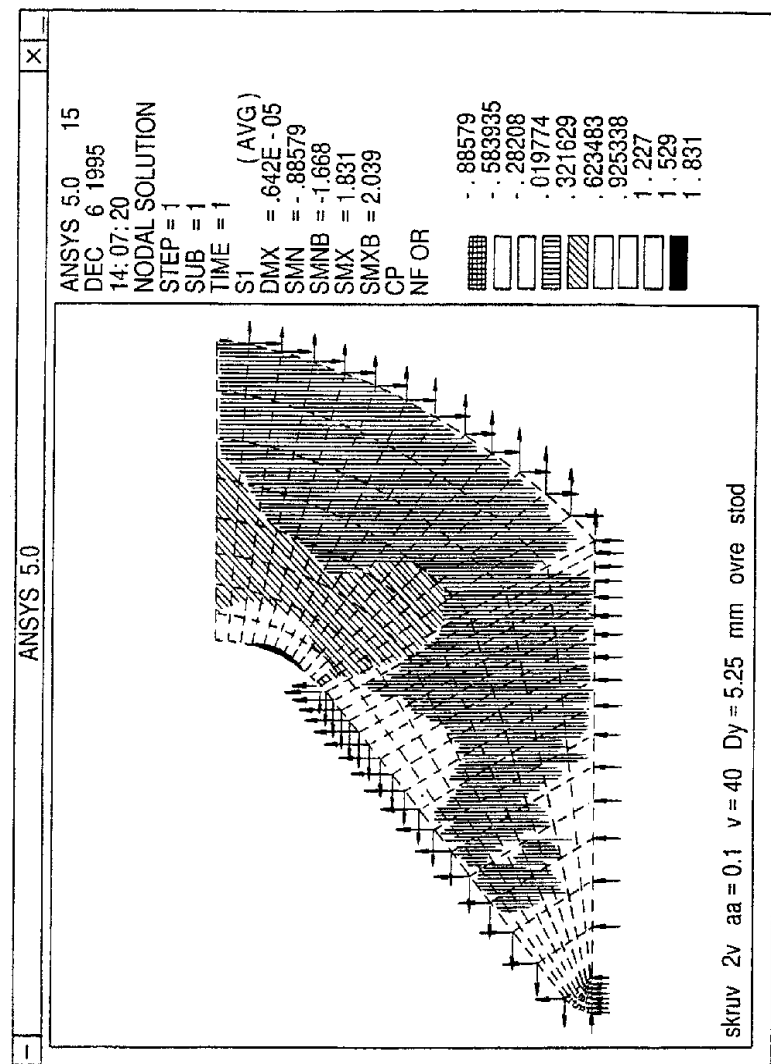


Fig.4

5/6

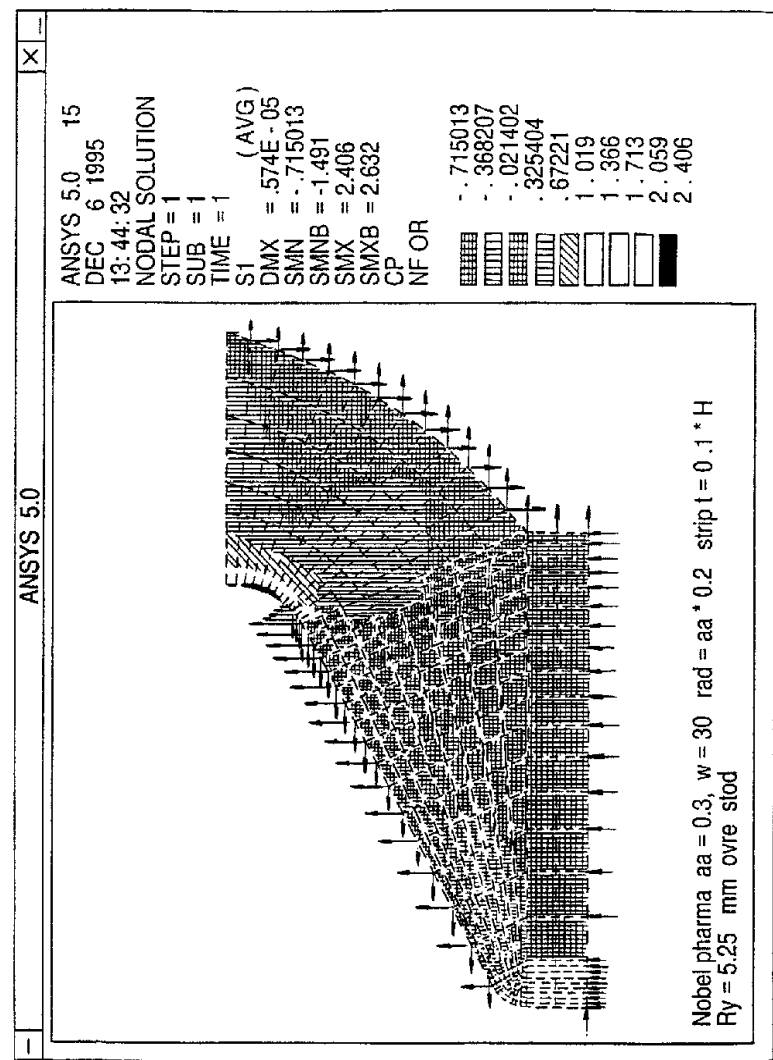


Fig.5

6/6

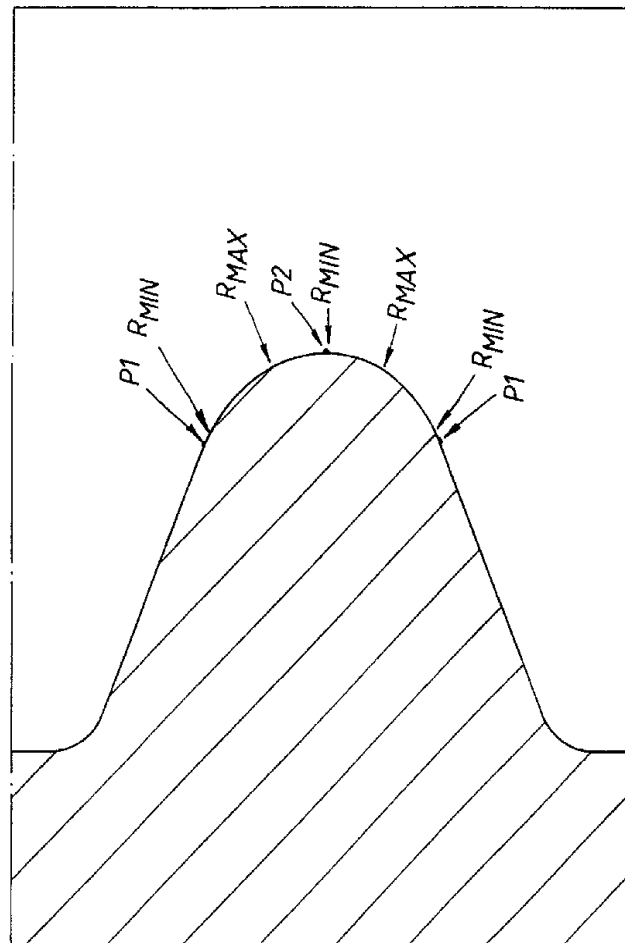


Fig.7